chemistry

MDPI

Article

The Preparation of Stable MoS_2 Dispersions by Using Well-Defined Polymers with Pendant Sulfide Moieties

Jin Motoyanagi *, Kohei Kawade and Masahiko Minoda *

Faculty of Molecular Chemistry and Engineering, Kyoto Institute of Technology, Graduate School of Science and Technology, Matsugasaki, Sakyo-ku, Kyoto 606-8585, Japan; kouheikawade78@gmail.com

* Correspondence: jinmoto@kit.ac.jp (J.M.); minoda@kit.ac.jp (M.M.); Tel.: +81-75-724-7537 (J.M.); +81-75-724-7513 (M.M.)

Abstract: The preparation of stable dispersions of MoS_2 by ultrasonic aqueous and/or organic media containing amphiphilic molecules is an attractive and widely applicable method to form MoS_2 fine particles while suppressing its aggregation. In this study, we developed a series of polymers with pendant sulfide moieties as a new dispersant, under the hypothesis that it would interact with sulfur atoms on MoS_2 surfaces. First, we designed a sulfide group-substituted methacrylate derivative (**ESMA**) with the hypothesis that it would interact with the MoS_2 surface through sulfur-sulfur interactions. Then, we synthesized well-defined polymers with pendant sulfide groups by living radical polymerization (ATRP). Next, 0.5 wt% MoS_2 was added to a DMSO solution containing 1 wt% of the obtained polymer (poly**ESMA**), and the mixture was treated with a bath-type ultrasonicator for 3 h to obtain a MoS_2 dispersion. We found that stable dispersions of MoS_2 in a fine particle state, although not in the form of single-layer or few-layer nanosheets, could be readily formed in DMSO using poly**ESMA** as a polymeric dispersant. Furthermore, we synthesized polymeric dispersants with different molecular weights and investigated the relationship between the structure of the dispersant and the dispersion stability.

Keywords: two-dimensional materials; molybdenum disulfide; ATRP; dispersion

check for updates

Academic Editors: Matthias Lehmann and Xiaodong Zhuang

Received: 11 March 2025
Revised: 12 April 2025
Accepted: 21 May 2025
Published: 23 May 2025

Citation: Motoyanagi, J.; Kawade, K.; Minoda, M. The Preparation of Stable MoS_2 Dispersions by Using Well-Defined Polymers with Pendant Sulfide Moieties. *Chemistry* **2025**, *7*, 84. https://doi.org/10.3390/chemistry7030084

Copyright: © 2025 by the authors. Licensee MDPI, Basel, Switzerland. This article is an open access article distributed under the terms and conditions of the Creative Commons Attribution (CC BY) license (https://creativecommons.org/licenses/by/4.0/).

1. Introduction

Recently, transition metal dichalcogenide (TMD) materials have garnered significant attention due to the unique properties exhibited by their layered structures. These compounds possess two-dimensional (2D) structures that display distinctive electrical, photonic, mechanical, and catalytic characteristics, which differ from those observed in three-dimensional (3D) bulk materials [1–5]. Especially, single-layer and few-layer molybdenum disulfides (MoS_2) have attracted significant attention due to their potential applications in various fields, including biosensors, photovoltaics, thermoelectric materials, supercapacitors, phototransistors, and hydrogen evolution catalysts [6–12]. Recently, considerable attention has been directed toward 2D MoS_2 due to its application as a luminescent material, exhibiting high luminescence efficiency when treated with super acids [13,14], and its use as an electrode material in rechargeable batteries [15,16]. Controlling the layer thickness of TMDs poses a significant challenge because their properties are sensitive to thickness variations. A variety of synthesis techniques have been developed, each of which can produce a product of a different amount, shape, and size. These techniques can be classified into the following two categories: (i) the bottom-up method, which assembles MoS_2 nanosheets using individual atoms, and (ii) the top-down method, where the properties of a sample evolve from a macroscopic size to a nanometric dimension (Figure 1) [17–19].

Various approaches such as chemical vapor deposition (CVD) and epitaxial growth techniques, one of the bottom-up methods, have been hitherto reported, and they successfully produced high-quality layered 2D MoS_2 nanosheets [9,20]. However, these methods require expensive equipment and limit the size of the nanosheets. On the other hand, Shear-assisted grinding and tape peeling methods, one of the top-down methods, also produced single- or few-layered MoS_2 nanosheets [21], but the quality was unsatisfactory and they were not easily scalable. Recently, ion-insertion chemical exfoliation methods using butyllithium or sodium naphthenate have been introduced by several research groups to scale up layered MoS_2 nanosheets [1,2,22]. However, these methods include laborious multi-step processes and are limited to being applicable only in aqueous media. The methodology for the prevention of the aggregation of single-layer or few-layers of 2D MoS_2 is well-established. This methodology involves the coating of the material with organic molecules. The following two coating methods have been identified: a covalent bond formation approach and a non-covalent bond approach. The covalent bond formation approach entails the coating of the surface with defects or SH sites on the MoS_2 surface, thereby forming covalent bonds with organic molecules [23,24]. Conversely, the non-covalent bond approach utilizes weak interactions, such as cation$-\pi$ interactions and electrostatic interactions, to coat the surface [25,26]. In recent years, the direct ultrasonic exfoliation of bulk MoS_2 in various solvents, such as NMP (*N*-methylpyrrolidone), acetonitrile, and water, together with dispersants [27–29], has been reported as an interesting approach to prepare single- or few-layered MoS_2. As polymeric dispersing agents, homopolymers with phosphonium salts and imidazolium salts in the side chains have been reported [30–32]. It is also known that amphiphilic triblock polymers consisting of poly(ethyleneoxide) and poly(propyleneoxide) (Pluronic®) function as dispersion stabilizers [33]. When reducing of the particle size of MoS_2, including exfoliating by using polymers as dispersants and external stimulus such as sonication, it is important to design polymeric molecules with a large number of functional groups that can multivalently interact with the surface of the MoS_2. Searching for such functional groups interacting with MoS_2 is an important issue for the preparation of stable dispersions of MoS_2 in a fine particle state or in a single- or few-layered state. In this study, we attempted to use a polymer with pendant sulfide moieties (poly**ESMA**) as a novel dispersant for MoS_2 (Figure 1). We expected that sulfur-sulfur interactions [34,35] would work between the sulfur atoms on the MoS_2 surface and the sulfide groups in the polymer side chains, and hence, the polymer would function as an effective dispersant. To this end, we synthesized a polymer (poly**ESMA**) with a well-defined structure by the controlled radical polymerization of a methacrylate monomer with a pendant sulfide group (**ESMA**). We then proceeded to evaluate the properties of the obtained polymers as a dispersant for MoS_2. Although no obvious exfoliation into single- or few-layered MoS_2 nanosheets was observed under the experimental conditions in this study, we succeeded in efficiently obtaining stable MoS_2 dispersions in a particle state through the appropriate molecular design of the polymeric dispersant, which is believed to be due to the MoS_2 particle surfaces being covered with the coexisting polymers through the interaction between the sulfide groups in the polymer side chains and the MoS_2 surfaces. In the previous study, we examined the formation of dispersions of carbon nanotubes by utilizing star-shaped polyphilic polymers as dispersants. It revealed that the degree of polymerization of the arm polymers of the star polymer exhibited a substantial influence on the dispersion stability [36]. Therefore, further investigation was conducted to explore the correlation between the molecular weight of the dispersant polymer (poly**ESMA**) and the dispersion ability for MoS_2.

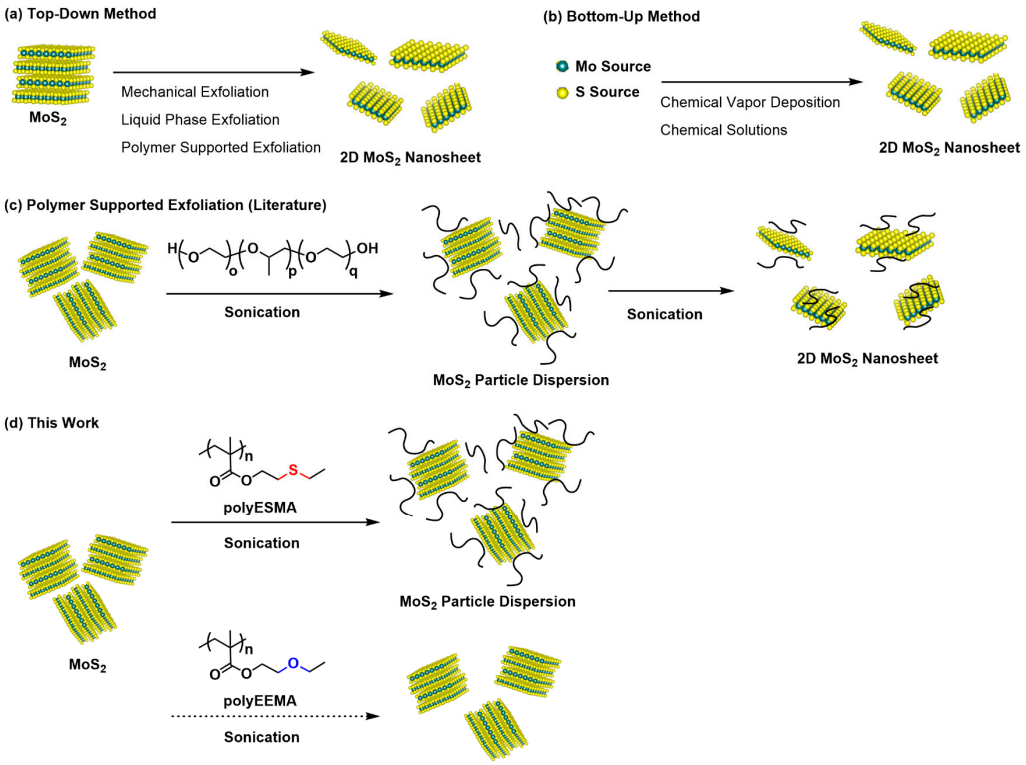


Figure 1. Illustration of the preparation of a 2D MoS_2 nanosheet by two approaches: (**a**) top-down method and (**b**) bottom-up method. The polymer-supported exfoliation of MoS_2 for the preparation of a 2D MoS_2 nanosheet using amphiphilic polymers [33] is illustrated in (**c**), and the preparation of a MoS_2 particle dispersion using the polymeric dispersant with pendant sulfide moieties (poly**ESMA**) is shown in (**d**). In this study, the formation of a MoS_2 nanoparticle dispersion was confirmed, but it was not verified that the nanoparticles were 2D sheets (see Results and Discussion); therefore, the figure shows the dispersed state of MoS_2 nanoparticles.

2. Materials and Methods

2.1. Chemicals and Reagents

Unless otherwise stated, all commercial reagents, including Ethyl 2-bromoisobutyrate (**EBIB**; Sigma-Aldrich Co., LLC., St. Louis, MO, USA, 98%), CuBr (FUJIFILM Wako Pure Chemical Corporation, Osaka, Japan, 99.9%), 1,1,4,7,10,10-Hexamethyltriethylenetetramine (**HMTETA**; Tokyo Chemical Industry Co., Ltd., Tokyo, Japan, 98%), *N*,*N*,*N*′,*N*″,*N*″-pentamethyldiethylenetriamine (**PMDETA**; FUJIFILM Wako Pure Chemical Corporation, Osaka, Japan, 98%), and MoS_2 (Sigma-Aldrich Co., LLC., St. Louis, MO, USA, 98%), were used as received. 2-Ethoxyethyl methacrylate (**EEMA**; Tokyo Chemical Industry Co., Ltd., Tokyo, Japan, 98%) was distilled over CaH_2. A methacrylate derivative with a sulfide group, 2-(Ethylthio)ethyl 2-methyl-2-propenoate (**ESMA**), was synthesized according to the literature [37].

2.2. Methods

^{1}H NMR spectra were assessed in $CDCl_3$ at 25 °C on a Bruker model AC-500 spectrometer (Bruker, Billerica, MA, USA), operating at 500 MHz, where chemical shifts (δ in ppm) were determined with respect to non-deuterated solvent residues as internal standards. Analytical size exclusion chromatography (SEC) was performed at 40 °C, using 8.0 mm × 300 mm polystyrene gel columns (TOSOH-TSKgel H type × 2) on a TOSOH GPC-8320 system (TOSOH, Tokyo, Japan), equipped with a UV-8000 variable-wavelength UV-vis detector (TOSOH, Tokyo, Japan). The number-average molecular weight (M_n) and molecular weight distribution (M_w/M_n) were calculated from the chromatographs with

respect to 15 polystyrene standards (Scientific Polymer Products, Inc., Ontario, NY, USA; M_n = 580–670,000 g mol^{-1}, M_w/M_n = 1.01–1.07). UV-vis spectra were recorded using a quartz cell of 1 cm path length on a SHIMADZU Type UV-2550 spectrometer (SHIMADZU, Kyoto, Japan). Thermogravimetric analysis (TGA) was performed with a TA Instruments Discovery TGA 5500 (TA Instruments, New Castle, DE, USA) in the temperature range 100–600 °C with a heating rate of 10 °C/min under an air stream. Dynamic light scattering (DLS) measurements were performed on an Otsuka Electronics ELSZ-1000ZS (Otsuka Electronics Co., Ltd., Osaka, Japan). Scanning electron microscopy (SEM) images were observed using a JEOL JSM–7600F (JEOL, Akishima, Japan). Infrared (IR) spectra were recorded at 20 °C on a JASCO model FT/IR-610 Plus Fourier transform infrared spectrometer (JASCO, Hachioji, Japan).

*2.3. Synthesis of poly**ESMA***

Poly**ESMA** was synthesized by the atom transfer radical polymerization (ATRP) of **ESMA** with **EBIB** as an initiator and CuBr/**HMTETA** as the ATRP catalyst [37]. A typical example of the polymerization procedure is given below. To a solution of **ESMA** (0.88 g, 5.1 mmol), **EBIB** (26 mg, 0.13 mmol), and **HMTETA** (24 mg, 0.10 mmol) in anisole (3.4 mL), CuBr (21 mg, 0.15 mmol) was added, and the resulting solution was degassed by three freeze–pump–thaw cycles. The solution was heated at 60 °C for 87 h and quenched by rapid cooling. The reaction mixture was analyzed by SEC and ^{1}H NMR spectroscopy. The reaction mixture was evaporated to dryness and subjected to column chromatography (Al_2O_3, THF). The THF solution of the reaction mixture was poured into a large amount of methanol to precipitate the polymers and remove the unreacted monomers. The resultant polymer was collected by centrifugation and dried under reduced pressure. The isolated polymer structure was analyzed by ^{1}H NMR spectroscopy.

*2.4. Synthesis of poly**EEMA***

Poly**EEMA** was synthesized by the atom transfer radical polymerization (ATRP) of **EEMA** with **EBIB** as an initiator and CuBr/**PMDETA** as the ATRP catalyst. A typical example of the polymerization procedure is given below. To a solution of **EEMA** (0.82 g, 5.1 mmol), **EBIB** (26 mg, 0.13 mmol), and **PMDETA** (18 mg, 0.10 mmol) in anisole (3.4 mL), CuBr (21 mg, 0.15 mmol) was added, and the resulting solution was degassed by three freeze–pump–thaw cycles. The solution was heated at 60 °C for 87 h and quenched by rapid cooling. The reaction mixture was analyzed by SEC and ^{1}H NMR spectroscopy. The reaction mixture was evaporated to dryness and subjected to column chromatography (Al_2O_3, THF). The THF solution of the reaction mixture was poured into a large amount of methanol to precipitate the polymers and remove the unreacted monomers. The resultant polymer was collected by centrifugation and dried under reduced pressure. The isolated polymer structure was analyzed by ^{1}H NMR spectroscopy.

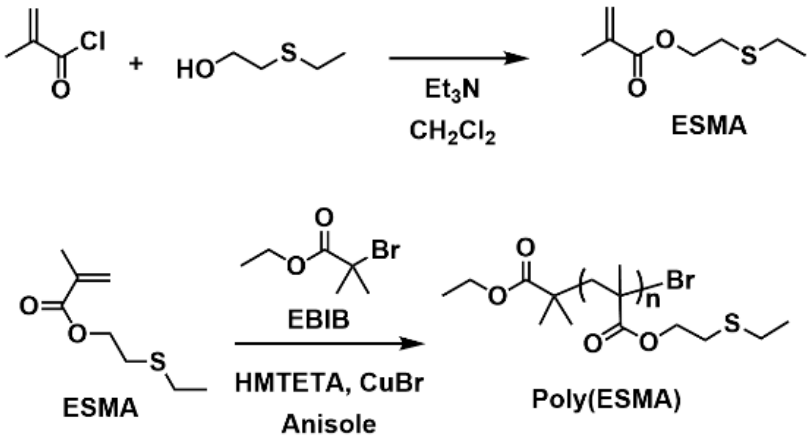
*2.5. Preparation of MoS_2 Dispersion with poly**ESMA** in DMSO*

To obtain dispersions of MoS_2, the following experimental protocol was used. First, a stock solution of 1 wt% poly**ESMA** in DMSO was prepared. MoS_2 powder (25 mg) was then added separately in 5 mL of polymer solution. The mixtures were sonicated continuously for 3 h using an Aiwa AU-80C ultrasonic bath (frequency 28 kHz). The temperature was maintained at 25 °C throughout the sonication period.

3. Results and Discussion

*3.1. Synthesis and Characterization of **ESMA** and poly**ESMA***

A methacrylate monomer with a sulfide group (**ESMA**) was obtained as a clear oil by the esterification of 2-(ethylthio)ethanol with methacryloyl chloride in CH_2Cl_2 at room temperature for 24 h in the presence of triethylamine (Scheme 1) [37]. We polymerized **ESMA** in anisole at 60 °C with **EBIB** under an ATRP condition ([**ESMA**]$_0$/[**EBIB**]$_0$/[CuBr]$_0$/[**HMTETA**]$_0$ = 50/1/1/1) (Scheme 1). After a period of 87 h, the polymerization was quenched (monomer conversion, 95%), and the resulting polymer was analyzed by size exclusion chromatography (SEC) using a refractive index (RI) detector in THF. The SEC curve of the obtained poly**ESMA** showed a unimodal peak (M_n = 7800, M_w/M_n = 1.20, estimated using polystyrene standards) (Figure 2). In the ^{1}H NMR spectrum (Figure 3), the peaks of the ethyl ester groups originating from the initiation terminal sites of poly**ESMA** overlapped with the peaks of the polymer side chains; thus, the signals assigned to the ethyl ester moieties of the obtained polymer were not observed as separate peaks. Because of the difficulty of calculating the number-average degree of polymerization (DP_n) of poly**ESMA** from ^{1}H NMR spectroscopy, the DP_n of poly**ESMA** was defined based on the feed molar ratio of **ESMA** to **EBIB** and the monomer conversion of 50 for convenience. Hereafter, this polymer with a theoretical DP_n of 50 is referred to as poly**ESMA**$_{50}$. By varying the polymerization conditions, we succeeded in the synthesis of poly**ESMA**s with different chain lengths (poly**ESMA**$_n$; the subscript n indicates the degree of polymerization, DP_n = 20, 25, 75, and 100). SEC analysis revealed that all the polymers of different DP_n values possessed well-controlled molecular weights (M_n) and molecular weight distributions (M_w/M_n) (Table 1).



Scheme 1. Synthesis of poly**ESMA**.

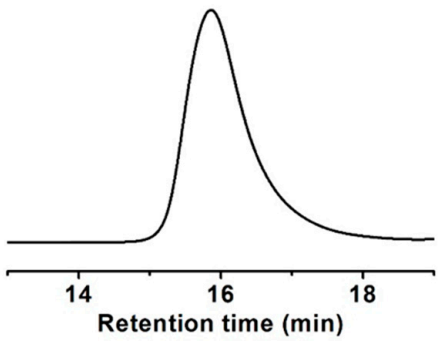


Figure 2. SEC curve of poly**ESMA** (theoretical DP_n = 50) measured in THF.

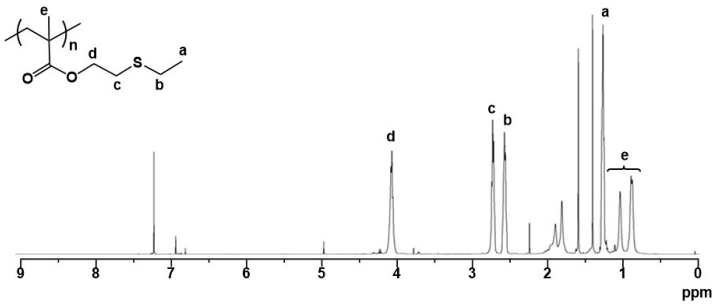


Figure 3. ^{1}H NMR spectrum of poly**ESMA** (theoretical DP_n = 50) in $CDCl_3$.

Table 1. Number-average degrees of polymerization (DP_n), molecular weights (M_n), and molecular weight distributions (M_w/M_n) of poly**ESMA**s.

	$[ESMA]_0/[EBIB]_0$	Conversion [a] (%)	DP_n [b]	M_n [c] (g mol^{-1})	M_w/M_n [c]
poly**ESMA**$_{50}$	50	95	50	7800	1.20
poly**ESMA**$_{20}$	25	84	20	6300	1.25
poly**ESMA**$_{25}$	25	99	25	7100	1.30
poly**ESMA**$_{75}$	85	88	75	13,800	1.16
poly**ESMA**$_{100}$	110	93	100	18,400	1.22
poly**EEMA**$_{50}$ [d]	50	88	50	8600	1.14

[a] Determined by ^{1}H NMR. [b] Theoretical DP_n calculated according to the following formula: DP_n = ([**ESMA**]$_0$/[**EBIB**]$_0$ × (conversion of **ESMA**). [c] Estimated by PSt-calibrated SEC in THF. [d] Synthesis of poly**EEMA** as a reference polymer by ATRP.

*3.2. Preparation of MoS_2 Dispersions with poly**ESMA** in DMSO*

To obtain the dispersion of MoS_2, we prepared 5 mL of DMSO solution of 1 wt% poly**ESMA**$_{50}$ with 25 mg of MoS_2, which was then sonicated for 3 h in a bath-type sonicator. This process yielded greenish dispersions (Figure 4), and to evaluate the stability of the resulting MoS_2 dispersion, a UV-vis spectrophotometer was used to measure the time-dependent changes in transmittance at 700 nm, a wavelength at which there is almost no absorption of MoS_2. The use of dispersant poly**ESMA**$_{50}$ resulted in minimal alterations in transmittance, even after a duration of 240 min, thereby indicating that a stable dispersion state was maintained by the polymer (Figure 4). In contrast, without any additives, MoS_2 rapidly aggregated and precipitated, resulting in a clear supernatant after 180 min. Furthermore, when the polymer with ether groups but without sulfide groups (poly**EEMA**; M_n = 7800, M_w/M_n = 1.20) was utilized as a reference additive, the supernatant also became clear after 180 min. This fact indicated that poly**EEMA** did not act as a dispersant for MoS_2. From these results, it is speculated that the sulfide groups on the polymer side chains interact with MoS_2 nanoparticles, enhancing the affinity of MoS_2 to the medium and improving the dispersion stability.

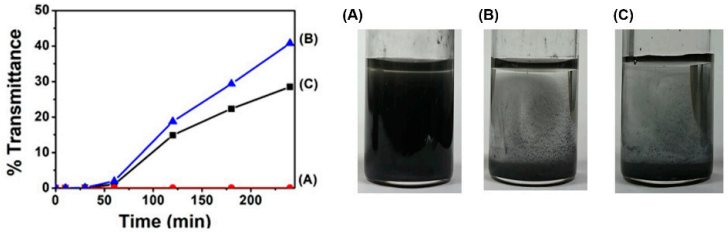


Figure 4. The transmittance changes (λ = 700 nm) of MoS_2 dispersions in DMSO and photographs of the MoS_2 dispersions in DMSO after 180 min of ultrasonic treatment and then, leaving them to stand for 240 min, the following were obtained: (**A**) with poly**ESMA**, (**B**) with poly**EEMA**, and (**C**) without any dispersant.

To analyze the dispersion state in more detail, dynamic light scattering (DLS) and scanning electron microscope (SEM) measurements of the dispersions and thermogravimetric analysis (TGA) measurements and infrared absorption spectrometry (IR) of the MoS_2 composite obtained by filtering the dispersion were carried out. We expected that DLS measurements would reveal whether the dispersed MoS_2 changed from its original size to a few-layer morphology. It was found that the dispersions examined in Figure 4 were highly concentrated, resulting in weak scattered light, preventing effective analysis. Therefore, the samples were diluted 10-fold in DMSO before performing DLS measurements. The measurement results shown in Figure 5 indicate that the size of MoS_2 particles was almost equal at about 400 nm when poly$ESMA_{50}$ was used as a dispersant and when no dispersant is added. This observation indicates that the addition of the dispersant did not exfoliate MoS_2 into single or few layers, but allowed for the formation of MoS_2 complexes through the interaction with poly**ESMA**$_{50}$ and resulted in stable dispersion formation. The morphological changes of MoS_2 were observed using SEM, and similar images were obtained regardless of the presence or absence of poly**ESMA**$_{50}$ (Figure 6). The SEM images are significantly different from those of MoS_2 exfoliated into a single layer or a few layer [38]. In consideration of the DLS measurement results, it was evident that MoS_2 did not undergo exfoliation during the dispersion process. Subsequently, the MoS_2 dispersion was filtered through a membrane filter, and the filtrate was subjected to TGA analysis (Figure 7) and IR analysis (Figure 8). The filtrate was thoroughly washed with ethanol and subsequently dried under vacuum conditions to obtain MoS_2 composites. When the MoS_2 composites were heated to 600 °C, a weight loss of approximately 2–3% was observed when poly**ESMA**$_{50}$ was used as a dispersant. In contrast, in the presence of poly**EEMA** or in the absence of any dispersing agent, no substantial disparities were discerned when subjected to analogous measurement conditions, with weight losses amounting to approximately 1% in both instances [39,40]. In the case of other MoS_2 composites with organic substances, when low molecular weight compounds were used and exfoliation into a single layer occurred, the weight loss was approximately 20% [41]. However, in this study, no exfoliation of MoS_2 was observed, and it was confirmed that the polymer covered the MoS_2 particles, which is presumably why only a slight weight loss was observed. In the IR measurement results of the MoS_2 composite, absorption due to the carbonyl stretching contained in the dispersant poly**ESMA**$_{50}$ was confirmed at approximately 1700 cm^{-1} (Figure 8). These observations are believed to be due to the formation of complexes between the MoS_2 particles and the organic material, poly**ESMA**, which contributes to the improved dispersion stability in DMSO.

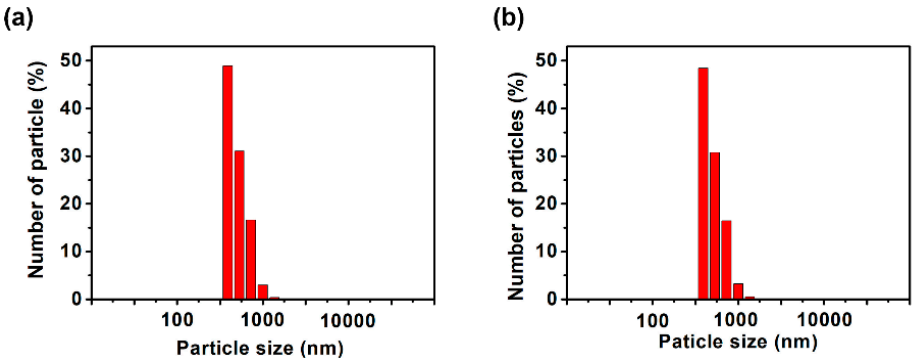


Figure 5. DLS analysis of MoS_2 dispersion formed (**a**) with poly**ESMA** and (**b**) without any dispersant. The samples were prepared by diluting the dispersion shown in Figure 4. 10 times with DMSO immediately before measurement.

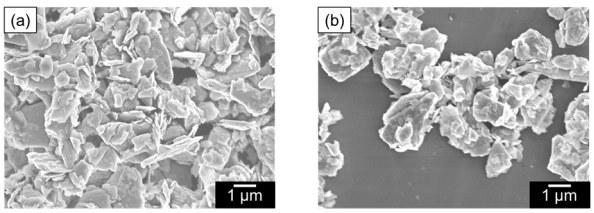


Figure 6. SEM images of (**a**) MoS_2 nanocomposites formed with poly**ESMA** and (**b**) MoS_2 powder.

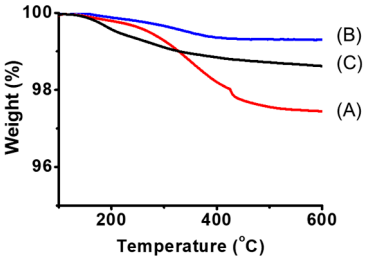


Figure 7. TGA curves of the measured samples derived from MoS_2 prepared with (A) poly**ESMA**, (B) poly**EEMA**, and (C) no dispersant.

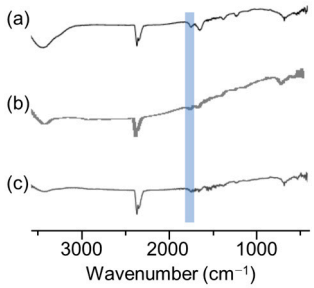


Figure 8. IR spectrum of MoS_2 composites with (a) poly**ESMA**, (b) poly**EEMA**, and (c) MoS_2 powder.

Subsequently, the relationship between the DP_n of poly**ESMA** and the dispersion stability was examined. Since poly**ESMA**s are synthesized by ATRP, a type of living radical polymerization, the DP_n of poly**ESMA** can be controlled by the feed ratio of monomer and initiator and the monomer conversion. The DP_n of poly**ESMA** synthesized in this study, as well as the M_n and M_w/M_n calculated by GPC analysis, are shown in Table 1. DMSO solutions (1 wt%), in amounts of 5 mL, of **ESMA** (monomer) and poly**ESMA**s with different DP_n were prepared, and MoS_2 was added then ultrasonicated. To compare the effect of DP_n of poly**ESMA** on the dispersion stability, the polymer concentration was set at 1 wt%, regardless of the degree of polymerization, and the concentrations of sulfide groups present in the dispersions were kept constant. By comparing the transmittance of the sample dispersions, it was observed that the stability of MoS_2 dispersions increased in proportion to the DP_n of poly**ESMA** in the range of DP_n from 1 (**ESMA** monomer) to 20, 25, and 50 (Figure 9a). Among these three polymers, poly$\mathbf{ESMA}_{50}$ provided the highest dispersion stabilization, whereas poly$\mathbf{ESMA}_{20}$ had the lowest dispersion stabilization ability, and its transmittance change over time was similar to that of the **ESMA** monomer (DP_n = 1). In addition, when poly$\mathbf{ESMA}_{25}$ was used as a dispersant, the MoS_2 dispersion was slightly stabilized, indicating that a decrease in the DP_n of poly**ESMA** resulted in a decrease in dispersion stabilization. These results were attributed to the fact that, as DP_n decreased, the number of sulfide groups in one polymer chain that could interact with sulfur atoms on the MoS_2 surfaces decreased, weakening the multivalent interaction, which is one of the polymer effects. When polymer samples with larger DP_n values were examined, it was very interesting to observe that the dispersion stability decreased as the DP_n increased in the

order of 50, 75, and 100 (Figure 9b). DLS measurements of MoS_2 dispersions obtained with poly**ESMA**s of different DP_n values demonstrated that the average particle size of MoS_2 remained virtually constant at 400 nm. This finding serves to confirm that the observed discrepancy in dispersion stability was not attributable to the size of the MoS_2 particles. This phenomenon may be due to the fact that, at high DP_n values, the molar concentration of poly**ESMA** decreases due to the increase in molecular weight, leading to a decrease in the number of poly**ESMA** molecules interacting with MoS_2.

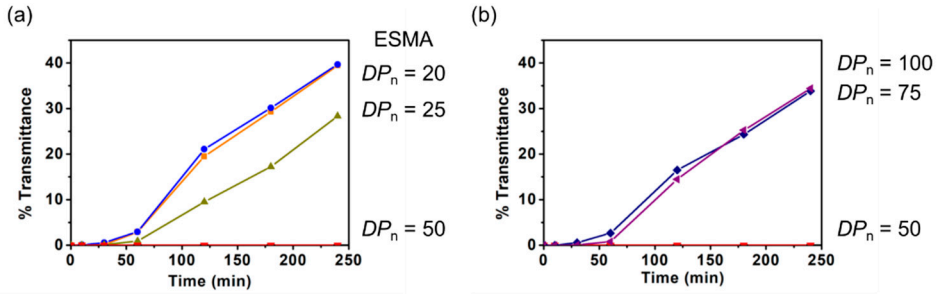


Figure 9. The transmittance changes (λ = 700 nm) of the MoS_2 dispersions in DMSO after 180 min of ultrasonic treatment with poly**ESMA**s and **ESMA** monomers. (**a**) The DP_ns are 1 (**ESMA** monomer), and 20, 25, and 50 for poly**ESMA**s. (**b**) The DP_ns of poly**ESMA** are 50, 75, and 100.

4. Conclusions

We demonstrated that stable dispersions of MoS_2 in a particle state in DMSO can be easily formed by using a polymer containing sulfide groups in the side chain (poly**ESMA**) as a polymer dispersant. We also clarified the effect of the DP_n of poly**ESMA** on the dispersion stabilization ability for MoS_2. These polymers are synthesized by ATRP, so there is a possibility that they can be copolymerized with other functional methacrylate monomers. In addition to controlling the DP_n, in the case of multicomponent polymers, for example, by controlling the combination and composition ratio of comonomers, they can be widely expanded to polyphilic derivatives, which would be significant as novel dispersants for chalcogenides in various media.

Author Contributions: Conceptualization, J.M. and M.M.; methodology, J.M. and M.M.; validation, J.M.; formal analysis, K.K.; investigation, J.M.; resources, J.M. and M.M.; data curation, K.K. and J.M.; writing—original draft preparation, J.M.; visualization, J.M.; supervision, M.M.; project administration, J.M.; funding acquisition, J.M. and M.M. All authors have read and agreed to the published version of the manuscript.

Funding: This research was funded by the JSPS KAKENHI, Grant-in-Aid for Scientific Research (C), grant numbers 20K05605 and 22K05216.

Data Availability Statement: Data are contained within the article.

Conflicts of Interest: The authors declare no conflicts of interest.

References

1. Eda, G.; Yamaguchi, H.; Voiry, D.; Fujita, T.; Chen, M.W.; Chhowalla, M. Photoluminescence from Chemically Exfoliated MoS_2. *Nano Lett.* **2011**, *11*, 5111–5116. [CrossRef] [PubMed]
2. Fan, X.B.; Xu, P.T.; Zhou, D.K.; Sun, Y.F.; Li, Y.G.C.; Nguyen, M.A.T.; Terrones, M.; Mallouk, T.E. Fast and Efficient Preparation of Exfoliated 2H MoS_2 Nanosheets by Sonication-Assisted Lithium Intercalation and Infrared Laser-Induced 1T to 2H Phase Reversion. *Nano Lett.* **2015**, *15*, 5956–5960. [CrossRef] [PubMed]
3. Huang, Y.; Sutter, E.; Shi, N.N.; Zheng, J.B.; Yang, T.Z.; Englund, D.; Gao, H.J.; Sutter, P. Reliable Exfoliation of Large-Area High-Quality Flakes of Graphene and Other Two-Dimensional Materials. *ACS Nano* **2015**, *9*, 10612–10620. [CrossRef] [PubMed]
4. Nicolosi, V.; Chhowalla, M.; Kanatzidis, M.G.; Strano, M.S.; Coleman, J.N. Liquid Exfoliation of Layered Materials. *Science* **2013**, *340*, 1226419. [CrossRef]

5. Niu, L.Y.; Coleman, J.N.; Zhang, H.; Shin, H.; Chhowalla, M.; Zheng, Z.J. Production of Two-Dimensional Nanomaterials via Liquid-Based Direct Exfoliation. *Small* **2016**, *12*, 272–293. [CrossRef]
6. Li, Y.F.; Liang, Y.L.; Robles Hernandez, F.C.R.; Deog Yoo, H.D.; An, Q.Y.; Yao, Y. Enhancing Sodium-Ion Battery Performance with Interlayer-Expanded MoS_2-PEO Nanocomposites. *Nano Energy* **2015**, *15*, 453–461. [CrossRef]
7. Sarkar, D.; Liu, W.; Xie, X.; Anselmo, A.C.; Mitragotri, S.; Banerjee, K. MoS_2 Field-Effect Transistor for Next-Generation LabelFree Biosensors. *ACS Nano* **2014**, *8*, 3992–4003. [CrossRef]
8. Wi, S.; Kim, H.; Chen, M.; Nam, H.; Guo, L.J.; Meyhofer, E.; Liang, X. Enhancement of Photovoltaic Response in Multilayer MoS_2 Induced by Plasma Doping. *ACS Nano* **2014**, *8*, 5270–5281. [CrossRef]
9. Wu, J.; Schmidt, H.; Amara, K.K.; Xu, X.; Eda, G.; Ozyilmaz, B. Large Thermoelectricity via Variable Range Hopping in Chemical Vapor Deposition Grown Single-Layer MoS_2. *Nano Lett.* **2014**, *14*, 2730–2734. [CrossRef]
10. Acerce, M.; Voiry, D.; Chhowalla, M. Metallic 1T Phase MoS_2 Nanosheets as Supercapacitor Electrode Materials. *Nat. Nanotechnol.* **2015**, *10*, 313–318. [CrossRef]
11. Li, H.; Wu, J.; Yin, Z.; Zhang, H. Preparation and Applications of Mechanically Exfoliated Single-Layer and Multilayer MoS_2 and WSe_2 Nanosheets. *Acc. Chem. Res.* **2014**, *47*, 1067–1075. [CrossRef] [PubMed]
12. Cummins, D.R.; Martinez, U.; Sherehiy, A.; Kappera, R.; Martinez-Garcia, A.; Schulze, R.K.; Jasinski, J.; Zhang, J.; Gupta, R.K.; Lou, J.; et al. Efficient Hydrogen Evolution in Transition Metal Dichalcogenides via a Simple One-Step Hydrazine Reaction. *Nat. Commun.* **2016**, *7*, 11857. [CrossRef] [PubMed]
13. Amani, M.; Lien, D.-H.; Kiriya, D.; Xiao, J.; Azcatl, A.; Noh, J.; Madhvapathy, S.R.; Addou, R.; Kc, S.; Dubey, M.; et al. Near-Unity Photoluminescence Quantum Yield in MoS_2. *Science* **2015**, *350*, 1065–1068. [CrossRef]
14. Molas, M.R.; Gołasa, K.; Bala, Ł.; Nogajewski, K.; Bartos, M.; Potemski, M.; Babiński, A. Tuning carrier concentration in a superacid treated MoS_2 monolayer. *Sci. Rep.* **2019**, *9*, 1989. [CrossRef]
15. Bhoyate, S.; Mhin, S.; Jeon, J.-E.; Park, K.R.; Kim, J.; Choi, W. Stable and High-Energy-Density Zn-Ion Rechargeable Batteries Based on a MoS_2-Coated Zn Anode. *ACS Appl. Mater. Interfaces* **2020**, *12*, 27249–27257. [CrossRef]
16. Liang, Y.; Feng, R.; Yang, S.; Ma, H.; Liang, J.; Chen, J. Rechargeable Mg Batteries with Graphene-like MoS_2 Cathode and Ultrasmall Mg Nanoparticle Anode. *Adv. Mater.* **2011**, *23*, 640–643. [CrossRef]
17. Samy, O.; Zeng, S.; Birowosuto, M.D.; El Moutaouakil, A. A Review on MoS_2 Properties, Synthesis, Sensing Applications and Challenges. *Crystals* **2021**, *11*, 355. [CrossRef]
18. Ismail, K.B.M.; Arun Kumar, M.; Mahalingam, S.; Kim, J.; Atchudan, R. Recent Advances in Molybdenum Disulfide and Its Nanocomposites for Energy Applications: Challenges and Development. *Materials* **2023**, *16*, 4471. [CrossRef] [PubMed]
19. Saliba, M.; Atanas, J.P.; Howayek, T.M.; Habchi, R. Molybdenum disulfide, exfoliation methods and applications to photocatalysis: A review. *Nanoscale Adv.* **2023**, *5*, 6787–6803. [CrossRef]
20. Zhang, Y.; Chang, T.-R.; Zhou, B.; Cui, Y.-T.; Yan, H.; Liu, Z.; Schmitt, F.; Lee, J.; Moore, R.; Chen, Y. Direct Observation of the Transition from Indirect to Direct Bandgap in Atomically Thin Epitaxial $MoSe_2$. *Nat. Nanotechnol.* **2014**, *9*, 111–115. [CrossRef]
21. Zhao, J.; Yu, H.; Chen, W.; Yang, R.; Zhu, J.; Liao, M.; Shi, D.; Zhang, G. Patterned Peeling 2D MoS_2 off the Substrate. *ACS Appl. Mater. Interfaces* **2016**, *8*, 16546–16550. [CrossRef] [PubMed]
22. Zheng, J.; Zhang, H.; Dong, S.H.; Liu, Y.P.; Nai, C.T.; Shin, H.S.; Jeong, H.Y.; Liu, B.; Loh, K.P. High Yield Exfoliation of Two Dimensional Chalcogenides Using Sodium Naphthalenide. *Nat. Commun.* **2014**, *5*, 2995. [CrossRef] [PubMed]
23. Saha, D.; Angizi, S.; Darestani-Farahani, M.; Dalmieda, J.; Selvaganapathy, P.R.; Kruse, P. Tuning the Chemical and Mechanical Properties of Conductive MoS_2 Thin Films by Surface Modification with Aryl Diazonium Salts. *Langmuir* **2022**, *38*, 3666–3675. [CrossRef] [PubMed]
24. Chou, S.S.; De, M.; Kim, J.; Byun, S.; Dykstra, C.; Jin Yu, J.; Huang, J.; Dravid, V.P. Ligand Conjugation of Chemically Exfoliated MoS_2. *J. Am. Chem. Soc.* **2013**, *135*, 4584–4587. [CrossRef]
25. Liu, W.; Yang, X.; Zhang, Y.; Xu, M.; Chen, H. Ultra-stable two-dimensional MoS_2 solution for highly efficient organic solar cells. *RSC Adv.* **2014**, *4*, 32744–32748. [CrossRef]
26. Tian, R.; Jia, X.; Lan, M.; Wang, S.; Li, Y.; Yang, J.; Shao, D.; Feng, L.; Su, Q.; Song, H. Ionic Liquid Crystals Confining Ultrathin MoS_2 Nanosheets: A High-Concentration and Stable Aqueous Dispersion. *ACS Sustain. Chem. Eng.* **2022**, *10*, 4186–4197. [CrossRef]
27. Coleman, J.N.; Lotya, M.; O'Neill, A.; Bergin, S.D.; King, P.J.; Khan, U.; Young, K.; Gaucher, A.; De, S.; Smith, R.J.; et al. Two Dimensional Nanosheets Produced by Liquid Exfoliation of Layered Materials. *Science* **2011**, *331*, 568–571. [CrossRef]
28. Dong, L.; Lin, S.; Yang, L.; Zhang, J.J.; Yang, C.; Yang, D.; Lu, H.B. Spontaneous Exfoliation and Tailoring of MoS_2 in Mixed Solvents. *Chem. Commun.* **2014**, *50*, 15936–15939. [CrossRef]
29. Jawaid, A.; Nepal, D.; Park, K.; Jespersen, M.; Qualley, A.; Mirau, P.; Drummy, L.F.; Vaia, R.A. Mechanism for Liquid Phase Exfoliation of MoS_2. *Chem. Mater.* **2016**, *28*, 337–348. [CrossRef]
30. Biswas, Y.; Dule, M.; Mandal, T.K. Poly(ionic liquid)-Promoted Solvent-Borne Efficient Exfoliation of MoS_2/$MoSe_2$ Nanosheets for Dual-Responsive Dispersion and Polymer Nanocomposites. *J. Phys. Chem. C* **2017**, *121*, 4747–4759. [CrossRef]

31. Wang, X.; Wu, P. Aqueous Phase Exfoliation of Two-Dimensional Materials Assisted by Thermoresponsive Polymeric Ionic Liquid and Their Applications in Stimuli-Responsive Hydrogels and Highly Thermally Conductive Films. *ACS Appl. Mater. Interfaces* **2018**, *10*, 2504–2514. [CrossRef] [PubMed]
32. Han, X.; Gao, J.; Chen, T.; Zhao, Y. Interfacial interaction and steric repulsion in polymer-assisted liquid exfoliation to produce high-quality graphene. *Chem. Pap.* **2020**, *74*, 757–765. [CrossRef]
33. Feng, X.; Xing, W.; Yang, H.; Yuan, B.; Song, L.; Hu, Y.; Liew, K.M. High-Performance Poly(ethylene oxide)/Molybdenum Disulfide Nanocomposite Films: Reinforcement of Properties Based on the Gradient Interface Effect. *ACS Appl. Mater. Interfaces* **2015**, *7*, 13164–13173. [CrossRef]
34. Kobayashi, K.; Masu, H.; Shuto, A.; Yamaguchi, K. Control of face-to-face π–π stacked packing arrangement of anthracene rings via chalcogen-chalcogen, Interaction: 9,10-bis(methylchalcogeno)anthracenes. *Chem. Mater.* **2005**, *17*, 6666–6673. [CrossRef]
35. Silaghi-Dumitrescu, R.; Lupan, A. Weak sulfur-sulfur interactions between chemically-identical atoms. *Cent. Eur. J. Chem.* **2013**, *11*, 457–463. [CrossRef]
36. Motoyanagi, J.; Matsumoto, T.; Shiotani, T.; Miki, S.; Minoda, M. Amphiphilic Star Polymers Bearing a Triphenylene Core for Novel Dispersants of Carbon Nanotubes in Polar Media. *Chem. Lett.* **2016**, *42*, 609–611. [CrossRef]
37. Kameyama, T.; Takasu, A. A Vinyl Polymer Having Pendent Sulfones Prepared by Atom-Transfer Radical Polymerization of a Sulfide-Containing Methacrylate and Electrophoretic Transparent Coating on a Stainless-Steel Anode. *Polym. Chem.* **2015**, *6*, 4336–4342. [CrossRef]
38. Lamkaouane, H.; Ftouhi, H.; Richard-Plouet, M.; Gautier, N.; Stephant, N.; Zazoui, M.; Addou, M.; Cattin, L.; Bernède, J.C.; Mir, Y.; et al. Efficient and Facile Synthetic Route of MoO_3:MoS_2 Hybrid Thin Layer via Oxidative Reaction of MoS_2 Nanoflakes. *Nanomaterials* **2022**, *12*, 3171. [CrossRef]
39. Jiang, Y.; Wang, J.; Wu, J.; Zhang, Y. Preparation of high-performance natural rubber/carbon black/molybdenum disulfide composite by using the premixture of epoxidized natural rubber and cysteine-modified molybdenum disulfide. *Polym. Bull.* **2021**, *78*, 1213–1230. [CrossRef]
40. Kabir, M.H.; Dias, D.; Arole, K.; Bahrami, R.; Sue, H.-J.; Liang, H. Hydrophilized MoS_2 as Lubricant Additive. *Lubricants* **2024**, *12*, 80. [CrossRef]
41. Liu, Y.; Zhang, S.; He, Y.; Chen, C.; Zhang, C.; Xie, P.; Zhong, F.; Li, H.; Chen, J.; Li, Z. APTES Modification of Molybdenum Disulfide to Improve the Corrosion Resistance of Waterborne Epoxy Coating. *Coatings* **2021**, *11*, 178. [CrossRef]

Disclaimer/Publisher's Note: The statements, opinions and data contained in all publications are solely those of the individual author(s) and contributor(s) and not of MDPI and/or the editor(s). MDPI and/or the editor(s) disclaim responsibility for any injury to people or property resulting from any ideas, methods, instructions or products referred to in the content.